Changes in the Secondary Structure of Bovine Casein by Fourier Transform Infrared Spectroscopy: Effects of Calcium and Temperature[1]

ABSTRACT

Bovine casein submicelles and reformed micelles, produced by addition of Ca^{2+}, were examined by Fourier transform infrared spectroscopy at 15 and 37°C in aqueous salt solutions of K^+ and Na^+. Previous measurements of caseins, made in D_2O and in the solid form, can now be made in a more realistic environment of H_2O. When analyzed in detail, data obtained by Fourier transform infrared spectroscopy have the potential to show subtle changes in secondary structural elements that are associated with changes in protein environment. Electrostatic binding of Ca^{2+} to casein resulted in a redistribution of the components of the infrared spectra. Addition of Ca^{2+} in salt solutions of K^+ and Na^+ led to apparent decreases in large loop or helical structures at 37°C with concomitant increases in the percentage of structures having greater bond energy, such as turns and extended helical structures. At 15°C, Na^+ and K^+ have differential effects on the Ca^{2+}-casein complexes. All of these observations are in accordance with the important role of serine phosphate side chains as sites for Ca^{2+} binding in caseins and the swelling of the casein structure upon incorporation into reformed micelles at 37°C. This new open, hydrated structure is buttressed by a change in backbone as evidenced by a shift in absorbance to higher wave numbers (greater bond energies) as colloidal micelles are reformed.

(**Key words**: milk protein, casein, protein structure, Fourier transform infrared spectroscopy)

Abbreviation key: **FTIR** = Fourier transform infrared, **NMR** = nuclear magnetic resonance, **RMS** = root mean square.

INTRODUCTION

Casein micelles, which are colloidal complexes of protein and salts, function biologically to transport efficiently and to deliver protein, calcium, and phosphorus to the neonate (9, 10, 21, 23). In the absence of calcium, the micellar structure dissociates into casein submicelles, consisting of α_{s1}-, α_{s2}-, β-, and κ-CN. Addition of Ca^{2+} results in the reformation of model casein micelles from the hydrophobically associated casein submicelles through the calcium-protein side-chain salt bridges (4, 9, 10). These calcium-protein interactions have been thought to involve both phosphate and carboxylate groups (9, 15). Studies using ^{31}P nuclear magnetic resonance (**NMR**) have been used to investigate the effects of Ca^{2+} on serine phosphate groups, which were shown to be primarily involved in the binding of calcium in solution (13); Fourier transform infrared (**FTIR**) spectroscopy has provided direct evidence for calcium binding to the negatively charged carboxylate groups of glutamate and aspartate residues in freeze-dried casein (1). With the use of laser Raman spectroscopy, the average relative conformations of individual caseins have been estimated in D_2O and under micellar and submicellar conditions in freeze-dried samples (2). The FTIR measurements of proteins were previously made in the solid state or in D_2O (27) in order to avoid the interference of water absorption with the absorbance of the secondary structure in the amide I region. These measurements can now be made in water with the use of extremely short path lengths and accurate water vapor subtraction (6, 7, 8). Measurements in aqueous solution should provide a more biologically realistic picture of Ca^{2+}-protein interactions by following changes in the components of the amide I and II regions of the spectra. Aqueous measurements also allow for the introduction of other ions, such as Na^+ and K^+, to create a biologically relevant environment in which to examine interactions and to estimate secondary structural changes.

We have used FTIR of aqueous solutions of casein submicelles and reformed micelles in the presence of sodium and potassium at two different temperatures: 15 and 37°C. The spectra have been analyzed with the use of Fourier smoothing of their second derivatives, followed by curve-fitting techniques to assess changes in components of the amide I and II regions. Such changes in these regions are correlated with components of protein secondary structure and with known changes of the sodium, potassium, and calcium caseinate system in water.

MATERIALS AND METHODS

Sample Preparation

Fresh, uncooled milk was obtained from a single Holstein cow and was treated immediately after collection with phenylmethylsulfonyl fluoride (0.1 $g \cdot L^{-1}$), a serine protease inhibitor, to retard proteolysis. The milk was transported to the laboratory and defatted twice by centrifugation at 4000 × *g* for 10 min at room temperature (23°C). The skimmed milk was diluted 1:1 (vol/vol) with distilled water and warmed to 37°C. Casein was precipitated by careful addition of 1*N* HCl to pH 4.6. The precipitate was homogenized (model ST-10; Polytron, Brinkman, Westbury, NY) at low speed, dissolved by addition of NaOH to give a solution of pH 7.0, reprecipitated, washed at 37°C and pH 4.6, and again resuspended at pH 7.0. This sodium caseinate suspension was subsequently cooled to 4°C and centrifuged at 10,000 × *g* for 30 min to remove residual fat and then freeze-dried. Alkaline urea-gel electrophoresis with standard caseins of known structure showed that the cow was of genotype α_{s1}-CN BB, β-CN AA, and κ-CN AA (24).

The lyophilized sodium caseinate was dissolved in 25 m*M* PIPES buffer (piperazine-N,N′-bis (2-ethanesulfonic acid)), pH 6.75, containing 110 m*M* KCl or NaCl. To produce model colloidal casein micelles (4, 17), a stock solution of $CaCl_2$ was added for a final concentration of 10 m*M*; KCl or NaCl was concomitantly reduced to 80 m*M* to maintain constant ionic strength. Casein concentrations, determined spectrophotometrically, ranged from 30 to 35 mg/ml (13).

Infrared Measurements

The submicellar and micellar bovine caseins were introduced into a demountable cell with CaF_2 windows and a 9- to 12-μm teflon spacer for H_2O. Spectra were obtained using an FTIR spectrometer (Nicolet 740; Madison, WI) equipped with a Nicolet 660 data system. Following purging of the sample chamber with N_2 to reduce water vapor to a minimum, data collection was carried out with each spectrum consisting of 4096 double-sided interferograms, coadded, phase-corrected, apodized (Happ-Genzel function), and fast Fourier transformed. The nominal instrument resolution was 2 cm^{-1} with one data point every 1 cm^{-1}. Absorption of the water vapor was routinely subtracted (6, 7, 8).

Data Analysis

Detailed descriptions of the methods of data capture, reduction, and analysis have been given (18) along with a corresponding basis set of globular proteins of known structure. This method was applied to the caseins. Briefly, protein spectra were obtained by subtraction of the buffer absorption from the respective solution absorption and then were used to calculate second-derivative spectra. These latter spectra served as a sensitive indication for identifying individual peak positions for subsequent processing. Then, as described by Kumosinski and Unruh (18), the spectra were fitted with Gaussian components (the positions were correlated with the second-derivative spectra) to yield fits, the root mean square (**RMS**) values of which were equivalent to or less than the baseline noise of the instrument. Finally, the fractional areas for the individual bands in the amide I and II regions of the spectra were calculated.

All spectra were fitted using a Gauss-Newton nonlinear iterative curve-fitting program[3] (5), which assumes Gaussian band envelopes for the resolved components. The three parameters of each band (height, peak frequency, and half-width plus half-height) were allowed to float during the iterations, as was the baseline. Integrated areas were calculated for those peaks that correspond to conformational elements, such as helices, sheets, turns, and loops (14, 18, 20, 26). This procedure yielded the relative areas of the components, which served to estimate the fraction of the various secondary elements in the protein molecule.

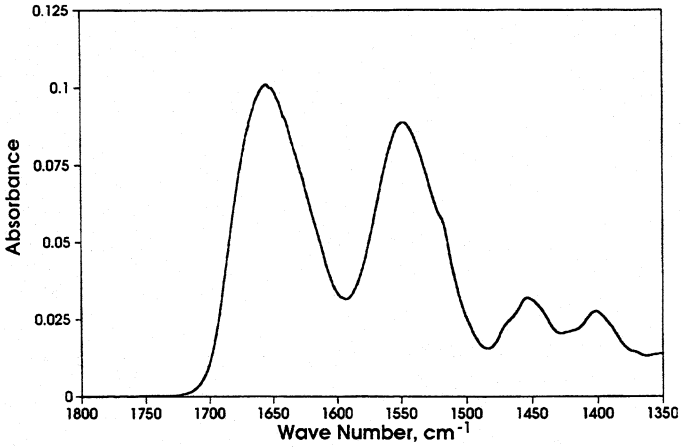

Figure 1. Original spectrum of casein (30 to 35 mg/ml) in 25 m*M* PIPES buffer, pH 6.75, in the presence of $CaCl_2$ (10 m*M*) at 37°C with KCl.

RESULTS

Original and Second-Derivative Spectra

Figure 1 shows the original spectrum of reformed bovine casein micelles in the presence of K^+ and Ca^{2+} at 37°C from 1800 to 1350 cm^{-1}. This spectrum is typical of all spectra that were obtained for the caseins and consists primarily of the amide I region, 1700 to 1600 cm^{-1}, and the amide II region, 1600 to 1500 cm^{-1}. The amide I region is mainly C=O stretching vibrations, and the amide II region is mainly N-H bending and C-N stretching modes. Little detail was observed in the amide I or amide II envelopes. In all cases, few differences were noted except for slight shifts in the frequencies of the amide I region with a change in the concentration of Ca^{2+}, temperature (data not shown), or both. On average, these shifts amounted to about 2 cm^{-1} in each case. When the second-derivative spectra of two samples were compared (Figure 2), overlapping bands could be visualized. For example, at 37°C and going from K^+ to K^+ + Ca^{2+}, a major band centering at 1639 cm^{-1} is relatively unchanged (Figure 2); bands between 1658 and 1652 cm^{-1} are shifted, rearranged, or dampened. Similarly, Ca^{2+} induced rearrangements also occur between 1630 and 1620 cm^{-1} with a diminution of these bands (Figure 2).

Fits to Spectra and Peak Assignments

Because the amide I envelopes are broad and not detailed and because the second-derivative spectra are qualitative in nature, quantitation of the changes was achieved through curve fitting of the amide I and II envelopes. In accordance with the procedures developed in this laboratory for a basis set of globular proteins (18), the spectra were fitted with Gaussian bands. The fitted spectra are typical of the curve fits of the amide I and II envelopes with an optimal number of components (18, 19). Peak positions in the curve fits were based on those found in the respective second-derivative spectra; however, floating of these values during the iteration process changed the positions slightly (<2 cm^{-1}). Optimal fits were supported by favorable RMS values on the order of 10^{-4}, which were less than the baseline noise. Figure 3 shows the results of a typical curve fit starting with wave numbers that were derived from the second derivative analysis. The fits to all spectra were adequate and had average RMS values in the range of 10^{-4}.

Peak assignments were made tentatively using the results of Krimm and Bandekar (14) as a primary guide, and refinements were based upon experimental data that had been collected for globular proteins (18, 19). For the amide I region, the following structures were assigned: turns, 1700 to 1660 cm^{-1}; α-helix, 1652 to 1648 cm^{-1}; irregular structures, 1648 to 1642 cm^{-1}; and β-sheet or nonstranded extended structure, 1640 to 1620 cm^{-1}. Upon data reduction (Figure 3), all casein spectra contained bands centering on 1656 cm^{-1}; such bands might be attributed theoretically to elements of α-helix or β-turns (14). However, NMR structural studies of the α_{s1}-CN peptide (f 59-79) demonstrated large loop structures for the

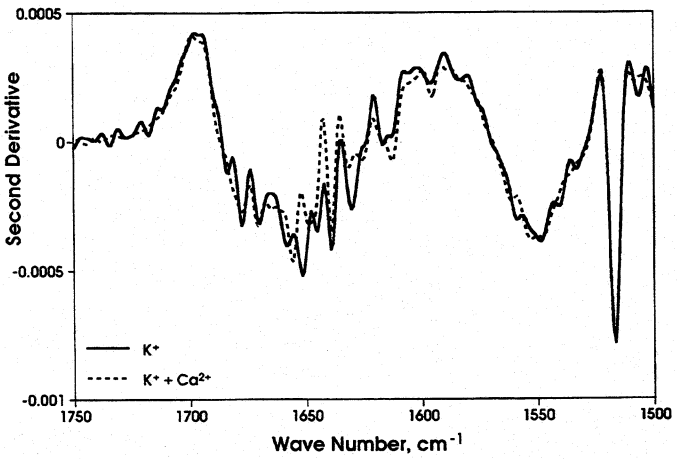

Figure 2. Second-derivative spectra of casein (30 to 35 mg/ml) in 25 m*M* PIPES buffer, pH 6.75, in the presence of K+/(80 m*M*) and $CaCl_2$ (10 m*M*) at 37°C or in the presence of KCl (110 m*M*) only. Both curves Fourier smoothed by a factor of 5. Frequency is given in wave numbers.

phosphoserine-containing segment (12). Similar structures, determined by NMR, have been reported for a β-CN peptide (25); thus, whole casein may contain loop-like structures. In addition, combined circular dichroism and FTIR experiments (26) have suggested that bands centered on 1656 cm^{-1} might arise from large loop structures rather than from α-helical structures. Accordingly, we placed the elements centering on 1656 cm^{-1} into a separate category termed large loops, which is not absolute evidence that the phosphopeptide directly gave rise to these bands, but rather, was done to establish a rationale for a separate category. In previous studies (2, 3) using Raman spectroscopy, such bands would have been counted as α-helix, perhaps overestimating the content of this structural element in the caseins. In a similar fashion, β-turns, γ-turns, and weak elements of β-sheet could all yield spectral components in the 1700 to 1670 cm^{-1} region (14). Additionally, Asn and Gln side chains, 3–10 helix, twisted sheet (18), and additional elements of β-turns (14) might give rise to components in the 1670- to 1660-cm^{-1} region. Because casein structures are not well characterized, we have summarized this region simply as turns.

For the amide II region, peak assignments were 1578 to 1555 cm^{-1} for turns, 1555 to 1543 cm^{-1} for α-helices or loops, and 1542 to 1525 cm^{-1} for β-sheets. Although our method enhances the resolution of the amide II region, the peaks generally overlapped to such an extent that assignments comparable with those of the amide I region were more difficult to make and, correspondingly, were more uncertain (18, 19). The errors associated with the integrated peak areas tended to be so large that the percentage of areas that were obtained were far less significant. However, the primary usefulness of the amide II region was to help to provide for a better fit of the amide I, particularly in the valley between the two peaks.

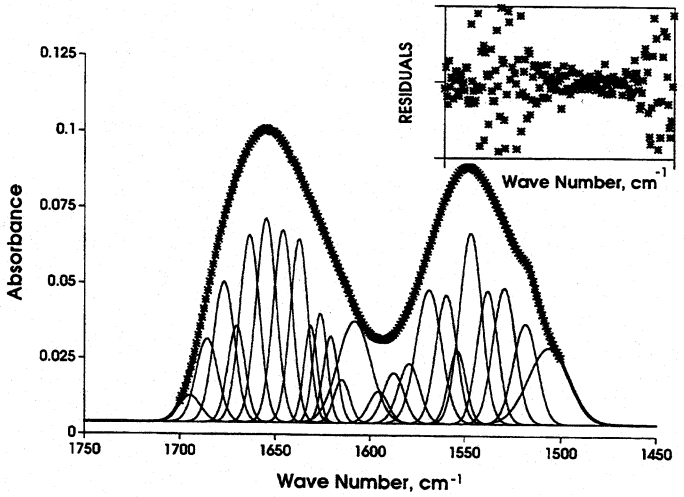

Figure 3. Original spectrum of casein (30 to 35 mg/ml) in 25 m*M* PIPES buffer, pH 6.75, in the presence of $CaCl_2$ (10 m*M*) at 37°C with KCl. Frequency in wave numbers. Amide I and II regions were fitted at peak positions obtained from second-derivative spectrum followed by Gaussian curve fitting (18, 19). Crosses represent experimental data; solid lines represent individual Gaussian components and their sum. Upper inset is the corresponding residual plot (ordinates in units of values ± 0.0003).

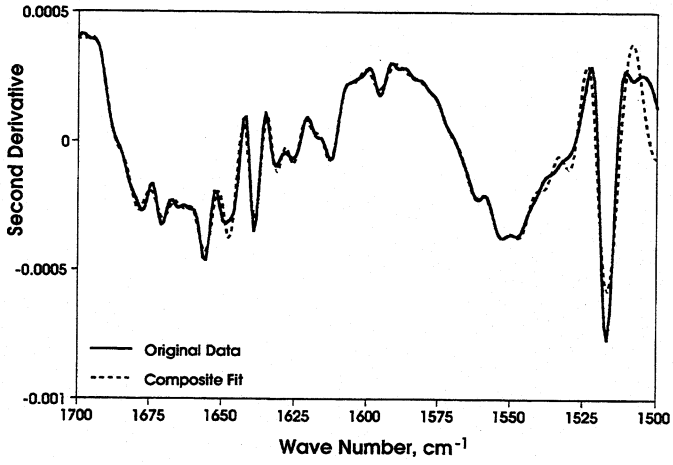

Figure 4. Second-derivative curve fit for the relative intensity of the spectra of casein (30 to 35 mg/ml) in 25 m*M* PIPES buffer, pH 6.75, in the presence of $CaCl_2$ (10 m*M*) at 37°C with KCl. Frequency is given in wave numbers. Solid line represents experimental data; dashed line represents second-derivative curves generated from the fitted data as in Figure 3. Both curves are Fourier smoothed using a factor of 5.

Fits to Original Spectra, Residual Plots, and Second Derivatives

Once the fits to the original spectra were obtained, two checks on the fitting routines were made. As a first measure of the quality of the fits, residual plots were obtained. These plots measure the quality of the fits and have distinctly random appearances (18, 19) for well-fitted spectra (inset, Figure 3). The residuals for the Gaussian fits to the spectra (inset, Figure 3) were typically random; the residuals lay between comparable values that were low, confirming the overall low RMS (10^{-4}) for the fits.

A second measure of the fitting procedure was obtained by overlaying the second derivative of the Gaussian summation (Figure 4) with the original

second derivative. Favorable RMS values were achieved for these fits as well. Figure 4 shows a typical overlay in which the second-derivative plot from the summation of the fitted areas of Figure 3 was compared with the second derivative of the original spectra. Good agreement between the two spectra suggests a good fit to the data.

Area Calculations and Redistribution of Structural Components

Areas that were calculated from nonlinear regression of the fitted spectra (Figure 3) may be considered to be proportional to the amounts of the conformational elements that were tentatively assigned (2, 3, 18, 19, 20). The tabulated areas with standard error and RMS of the fit were taken from the curve fits for each environmental condition (Tables 1 and 2). Table 3 summarizes the overall composite structures for the amide I region for each of the eight environmental conditions listed.

To help in understanding the effects of temperature and Ca^{2+} binding and the influence of Na^+ and K^+ on the caseins, the redistribution of selected bands (corresponding to possible conformational elements) was examined. For example, when the temperature of the submicelles was increased in the presence of K^+ from 15 to 37°C, no significant change was observed in the summed components (Table 3). However (at 37°C), the 1626 and 1633 cm^{-1} bands redistributed into two components, 1624 and 1631 cm^{-1} (Table 1). Thus, although the total β-sheet was not appreciably changed, the bands giving rise to it appeared to shift. At 37°C and in the presence of Ca^{2+} and K^+, a decrease in loop and helical structures occurred with a redistribution to turns (Table 3). The bands attributed to loop and helix (1658 and 1650 cm^{-1}) appeared to merge at 1654 cm^{-1}, and the areas of the bands at >1663 cm^{-1} increased. Thus, in Ca^{2+} at 37°C, there was an overall increase in turns at the possible expense of loop or helical structures (Table 3), which represents a movement to higher bond energies (14) caused by elevated temperature and Ca^{2+}.

In the presence of Na^+, the increase in temperature of the submicelles from 15 to 37°C did not significantly affect the component areas (Table 3). But, as was the case for the experiments using K^+, a redistribution of bands occurred that was attributed to β-sheet structures as the temperature increased (Table 2). On addition of Ca^{2+}, even at the lower temperature, turn components increased or possibly shifted to yield a band at 1668 cm^{-1}, accounting for 10.4% of the total area (Table 2). This band, although not promi-

TABLE 1. Amide I measured percentage peak areas.

Conformational element	K^+ at 15°C			K^+ at 37°C			K^+ and Ca^{2+} at 15°C			K^+ and Ca^{2+} at 37°C		
	Frequency	Area		Frequency	Area		Frequency	Area		Frequency	Area	
	(cm^{-1})	— (%) —		(cm^{-1})	— (%) —		(cm^{-1})	— (%) —		(cm^{-1})	— (%) —	
		$\bar{X}$	SE[1]		$\bar{X}$	SE[1]		$\bar{X}$	SE[1]		$\bar{X}$	SE[1]
Turn	1696	1.1	0.1	1695	1.8	0.4	1696	2.0	0.1	1694	2.3	0.1
Turn	1687	4.8	0.5	1688	3.4	0.8	1688	2.5	0.4	1685	6.9	0.8
Turn	1679	6.6	1.0	1683	3.5	0.8	1686	1.5	0.2	1677	11.3	2.2
Turn	1673	7.3	0.8	1678	8.2	1.2	1680	8.6	1.7			
Turn[2]	1667	7.6	1.9	1670	10.2	2.6	1672	10.6	1.9	1670	6.5	0.6
Turn[2]	1663	7.2	1.0	1664	6.9	1.0	1665	9.0	1.5	1663	14.4	2.2
Large loop[3]	1657	8.0	1.8	1658	14.2	2.8	1658	8.5	2.3	1654[4]	15.8	3.0
α-Helix	1650	16.1	1.6	1652	9.4	1.8	1650	21.1	2.0			
Irregular	1642	14.3	1.2	1645	12.1	2.0	1642	10.7	1.6	1646	14.2	1.7
β-Sheet[5]	1637	2.6	0.8	1638	7.6	1.0	1635	9.5	1.7	1638	12.8	0.9
β-Sheet[5]	1633	3.6	0.6	1631	15.5	2.1	1628	9.0	1.4	1631	5.0	1.8
β-Sheet[5]	1626	21.2	3.6	1624	6.7	1.7	1623	5.2	1.1	1626	5.8	1.1
β-Sheet[5]										1621	4.9	0.5
RMS[6]	3.4×10^{-4}			6.5×10^{-4}			2.6×10^{-4}			7.3×10^{-4}		

[1]Standard error calculated as by Kumosinski et al. (19) for reanalysis of the same sample.

[2]This band contains elements of amide side chains (Asn and Gln) as well as bent strand and 3–10 helix (18).

[3]This band was designated as arising from large loops (26), but may contain α-helical and β-turn elements (14).

[4]Unresolved loop and α-helix in the fitting routine.

[5]These elements include both stranded (hydrogen-bonded) sheet as well as unstranded (extended) sheet (14, 18).

[6]Root mean square of the fit.

nent in the Na^+ only fits, is comparable with components in the K^+ series. The band was retained and even increased slightly to 11.8% at 37°C. Previous theoretical calculations (14), as well as studies with globular proteins (18, 19), attribute such bands to β-turns, side chains, bent strands, or 3-10 helices. The α-helical structures and loops appeared to decrease at 37°C; the increase in resonances at higher wave numbers at both 15 and 37°C and with the addition of Ca^{2+} (Table 3) have been noted.

DISCUSSION

We have shown that the amide I region of the FTIR spectra for bovine casein submicelles and reformed micelles in aqueous salt solution can be studied and quantitated by a combination of second-derivative analysis and curve fitting. Our study yielded a global estimation of the various elements of the secondary structures (turns, α-helices, irregular structures, loops, and β-sheets) in the protein molecule that can report upon structural changes in a water environment, as opposed to previous studies with environments of solids or D_2O, (1, 2, 3). The casein submicellar structure, which is held together by predominantly hydrophobic forces, shows subtle changes when Ca^{2+} is added. Ion-binding of Ca^{2+} to the side chains results in overall conformational changes to the backbone. To date, binding has been shown to involve both the serine phosphates (9, 13) and the carboxyl groups of glutamate and aspartate residues in lyophilized samples (1). Temperature increases might cause additional changes in the backbone conformation because of concurrent increases in hydrophobic interactions. The influence of Na^+, and K^+, which are normally present in milks (9, 10, 21, 23), combined with these other effects and gave information on the environment in which these submicelles and reformed micelles exist.

Ca^{2+} Effects

In the K^+ and Na^+ solutions in the presence of Ca^{2+}, at higher temperatures, total α-helical and large loop structures decreased about 10%. When Ca^{2+} is added to the casein submicelles, colloidal casein structures are reformed under identical experimental conditions (4). Kakalis et al. (13) presented direct evidence using ^{31}P NMR that Ca^{2+} interacts with serine phosphate side chains in solution. If these side chain phosphates are located on large loops, as suggested by NMR studies of casein structure (12), then the electrostatic binding of Ca^{2+} and the subsequent formation of colloids could alter these structures. This influence is evident in the previously mentioned decreases in percentages of

TABLE 2. Amide I measured percentage peak areas.

Conformational element	Na^+ at 15°C			Na^+ at 37°C			Na^+ and Ca^{2+} at 15°C			Na^+ and Ca^{2+} at 37°C		
	Frequency	Area		Frequency	Area		Frequency	Area		Frequency	Area	
	(cm^{-1})	— (%) —		(cm^{-1})	— (%) —		(cm^{-1})	— (%) —		(cm^{-1})	— (%) —	
		$\bar{X}$	SE[1]		$\bar{X}$	SE[1]		$\bar{X}$	SE[1]		$\bar{X}$	SE[1]
Turn	1686	7.4	1.1	1687	5.9	0.1	1692	2.7	0.4	1693	3.0	0.4
Turn	1680	3.9	0.8	1680	9.0	0.9	1684	6.1	1.0	1686	3.5	1.2
Turn	1676	4.4	1.0				1680	2.7	1.0	1682	4.6	2.0
Turn	1671	5.8	0.8	1673	7.0	1.8	1675	7.9	2.0	1675	7.4	2.0
Turn[2]							1667	10.4	1.9	1668	11.8	2.3
Turn[2]	1664	14.9	2.4	1666	14.2	1.5	1661	9.4	1.9	1661	12.6	1.1
Large loop[3]	1657	15.5	0.7	1658	17.0	2.4	1655	10.2	2.0	1654[4]	9.7	2.0
α-Helix	1649	10.0	0.8	1649	10.8	1.7	1649	10.2	1.5	1650	9.3	1.6
Irregular	1643	8.7	2.1	1642	7.3	1.3	1644	8.4	2.2	1644	11.6	2.2
β-Sheet[5]	1637	11.9	1.8	1638	7.0	1.0	1638	9.8	1.1	1639	9.2	1.0
β-Sheet[5]	1628	11.1	2.0	1633	5.9	0.8	1631	10.0	2.1	1632	8.8	0.7
β-Sheet[5]	1622	7.0	2.0	1629	6.0	1.3	1624	4.6	0.9	1624	9.4	0.5
β-Sheet[5]				1624	6.3	1.0	1621	7.5				
RMS[6]	2.1×10^{-4}			4.3×10^{-4}			3.3×10^{-4}			2.4×10^{-4}		

[1]Standard error calculated as by Kumosinski et al. (19) and for reanalysis of the same sample.

[2]This band contains elements of amide side chains (Asn and Gln) as well as bent strand and 3-10 helix (18).

[3]This band was designated as arising from large loops (26), but may contain α-helical and β-turn elements (14).

[4]Unresolved α-helix and large loop structures in the fitting routine.

[5]These elements include both stranded (hydrogen-bonded) sheet as well as unstranded (extended) sheet (14, 18).

[6]Root mean square of the fit.

TABLE 3. Total estimated secondary contributions of amide I.

Conformational element	K^+ at 15°C	K^+ at 37°C		K^+ and Ca^{2+} at 15°C		K^+ and Ca^{2+} at 37°C
	Area	Area		Area		Area
	(%)	(%)	SE[1]	(%)	SE[2]	(%)
Total turn	34.6	34.0	1.2	34.2	3.2	41.4[a]
Total large loop and α-helix	24.1	23.6	1.8	29.6[a]	5.4	15.8[b]
Irregular	14.3	12.1	3.2	10.7	2.3	14.2
Total β-sheet	27.4	29.8	2.3	23.4	2.3	28.5
	Na^+ at 15°C	Na^+ at 37°C		Na^+ and Ca^{2+} at 15°C		Na^+ and Ca^{2+} at 37°C
Total turn	36.4	36.1	1.2	39.2[a]	3.2	42.9[b]
Total large loop and α-helix	25.5	27.8	1.8	20.4[a]	5.4	19.0[a]
Irregular	8.7	7.3	3.2	8.4	2.3	11.6
Total β-sheet	30.0	25.2	2.3	27.3	2.3	27.4

[a,b]Significantly different for the pooled means of the conformational element ($P > F = 0.05$ using a two-tailed distribution).

[1]Standard error for all summed data at 15 and 37°C in K^+ or Na^+; n = 4.

[2]Standard error for all summed data at 15°C and Ca^{2+} with K^+ or Na^+; n = 3 (one data set in K^+ not shown here).

structural components in 1658- to 1651-cm^{-1} bands at 37°C in the presence of Ca^{2+} with either electrolyte. In the experiment using K^+, the reformed micelles at 37°C exhibited an apparent increase in components, giving rise to bands at wave numbers >1660 cm^{-1}. For the experiment using Ca^{2+} + Na^+ at 37°C, similar effects also occurred at the lower temperature (15°C) when micelles are not completely reformed (Table 2).

The effects of Ca^{2+} on global protein structure with micelle formation has been suggested by several physical chemical studies (4, 10, 17). In particular, studies (17) employing small-angle X-ray scattering predicted a swelling of the outer shell of casein submicelles as they are incorporated into micelles. This swelling represented a 30% increase in hydration (with a concomitant decrease in the electron density of proteins). Holt and Sawyer (11) have suggested that a recurrent motif in ruminant caseins is α-helix-loop-α-helix in which the loop region is typically phosphorylated. Such motifs were also predicted by studies (16) using molecular modeling. Studies (15) of the molecular dynamics of the α_{s1}-CN phosphopeptide also suggested that the swelling of these loop structures accommodated the increased hydration that accompanied Ca^{2+} binding. Thus, presumably the Ca^{2+} binding and the incorporation of Ca^{2+} caseinates into micelles could deform α-helical elements and extend loop elements because they are spatially adjacent. Hence, the changes in the 1655 ± 5 cm^{-1} region upon Ca^{2+} addition could be due to loop-helix alterations with movement of the resonances to higher wave numbers and with the higher bond energies needed to buttress the swelling and extension of the polypeptide chains.

Temperature Effects

Under submicellar conditions (i.e., without added Ca^{2+}), casein undergoes a temperature-dependent hydrophobic aggregation to a limiting polymer with a molecular mass of approximately 250,000 Da (4, 10, 21, 23). At the concentrations used in these experiments (30 to 35 mg/ml), either the limiting polymer is maintained at both 15 and 37°C in the presence of Na^+ and K^+, or no gross change in the backbone structure occurs as a result of aggregation (Table 3). However, significant redistribution of component areas did occur within the larger categories (Tables 1 and 2). For example, the components of the β-sheet (extended structure) were redistributed between 15 and 37°C in the presence of either Na^+ or K^+ (Tables 1 and 2). These rearrangements are also detected in the second-derivative spectra (Figure 2) that were obtained in the presence of K^+ or K^+ with Ca^{2+}.

When Ca^{2+} was added, inducing colloid reformation (4), significant structural changes occurred for the samples at 37°C containing either Na^+ or K^+. As was noted, the structure of the phosphopeptide was sensitive to Ca^{2+} as was demonstrated by NMR (12, 13) and simulations of molecular dynamics (15). Additionally, a loop structure has been indicated by two-dimensional NMR (12). Several researchers [as reviewed in (9, 10, 21, 23)] have concluded that micelle formation is incomplete at 15°C and that the amount of serum casein is significantly reduced at 37°C. Thus, in the presence of Ca^{2+}, the secondary structural changes to higher energies (greater wave numbers) with increased temperature yielded more support for the increased open-hydrated structure observed by physical measurements (17). These changes are most likely the result of the reformation of colloidal micelles.

Salt Effects

Under submicellar conditions, switching from K^+ to Na^+ at either 15 or 37°C seemed to produce few changes (Table 3). Thus, under submicellar conditions, in the absence of Ca^{2+}, the replacement of Na^+, which has an ionic radius of 0.97 Å, with K^+, which has a radius of 1.3 Å, caused almost no gross conformational changes, but, again, some component elements of the classes of structure were redistributed (Tables 1 and 2).

For reformed micelles with added Ca^{2+} at 37°C, the replacement of Na^+ with K^+ appeared to yield similar overall results (Table 3); that is, there was a decrease in loop and helical structures with an increase in turns. Curiously, Na^+ and K^+ were different at 15°C in the presence of Ca^{2+} (Table 3). Although both Na^+ and K^+ might interact with casein, yielding little or no conformational change at 15 or 37°C when Ca^{2+} was not present, the changes might have caused a differential competition with Ca^{2+} in micelles that were incompletely reformed at 15°C. These regions of the spectra are also known to be where absorption of asparagine and glutamine occurs (18). Correction in these spectral regions of the peak areas for side-chain vibrations would have reduced the area values (17, 18); however, the relative reactivity of the α-helix-loop region would have been retained because the content of these side chains is constant.

Unfortunately, because bovine casein has never been crystallized, there is little information on its structure to date. In addition, proteins, such as casein, could have unique structural components that are not contained in our databases of globular proteins (18, 19). Byler and Farrell (1), Byler et al. (2), and Byler and Susi (3) have gathered some information through both Raman and infrared spectroscopies with which our data correlates fairly well. These researchers (1, 2, 3) worked with solid whole casein at room temperature, which may have different band assignments than our aqueous systems at 15 and 37°C. However, even when compared with their slightly different structural assignments, our results are similar. As disclosed here, FTIR offers a method for following structural changes that are introduced in solution by altering the temperature and electrolyte balance. The redistribution of components within classes of structure with changes in environment (Figure 2 and Tables 1 and 2) are reproducible, but the precise changes in the secondary structures that give rise to these bands are not known. Therefore, this information must be treated with caution as the relative assignments are tentative (14), based on a database of globular proteins (18, 19), and subject to changing interpretations (22). However, an examination of the second-derivative analyses of the primary data (Figure 2) clearly shows differences in the absorbances of amide I region under changing environmental conditions. These qualitative changes can now be used as the basis for quantitative analyses by use of nonlinear regression routines. The curve fitting and assignments, however tentative, can yield a measure of these differences and indicate molecular bases for these changes. This analysis would yield not only basic information, but also, as these FTIR measurements can now be made in H_2O (rather than D_2O), could be extended to yield information on actual food processing systems.

ACKNOWLEDGMENT

The authors thank John Phillips for his assistance with statistical analysis and the SAS program.

REFERENCES

1 Byler, D. M., and H. M. Farrell, Jr. 1989. Infrared spectroscopic evidence for calcium ion interaction with carboxylate groups of casein. J. Dairy Sci. 72:1719–1723.

2 Byler, D. M., H. M. Farrell, Jr., and H. Susi. 1988. Raman spectroscopic study of casein structure. J. Dairy Sci. 71: 2622–2629.

3 Byler, D. M., and H. Susi. 1986. Examination of the secondary structure of proteins by deconvolved FTIR spectra. Biopolymers 25:469–487.

4 Chu, B., Z. Zhou, G. Wu, and H. M. Farrell, Jr. 1995. Laser light scattering of model casein solutions: effects of high temperature. J. Colloid Interface Sci. 170:102–112.

5 Damert, W. 1994. A nonlinear regression program, Program 652. Quantum Chem. Progr. Exchange Bull. 14:61.

6 Dong, A., P. Huang, and W. S. Caughey. 1990. Protein secondary structures in water from second-derivative amide I infrared spectra. Biochemistry 29:3303–3308.

7 Dousseau, F., and M. Pezolet. 1990. Determination of the secondary structure content of proteins in aqueous solutions from their amide I and amide II infrared bands. Comparison between classical and partial least-squares methods. Biochemistry 29:8771–8779.

8 Dousseau, F., M. Therrien, and M. Pezolet. 1989. On the spectral subtraction of water from the FT-IR Spectra of aqueous solutions of proteins. Appl. Spectrosc. 43:538–542.

9 Farrell, H. M., Jr., and M. P. Thompson. 1988. Calcium binding proteins. Pages 117–132 *in* Caseins as Calcium Binding Proteins. Vol. 2. M. P. Thompson, ed. CRC Press, Inc., Boca Raton, FL.

10 Holt, C. 1992. Structure and stability of bovine casein micelles. Adv. Protein Chem. 43:63–151.

11 Holt, C., and L. Sawyer. 1988. Primary and predicted secondary structures of the caseins in relation to their biological functions. Protein Eng. 2:251–259.

12 Huq, N. L., K. J. Cross, and E. C. Reynolds. 1995. A ^{1}H-NMR study of the casein phosphopeptide α_{s1}-casein (59–79). Biochim. Biophys. Acta 1247:201–208.

13 Kakalis, L. T., T. F. Kumosinski, and H. M. Farrell, Jr. 1990. A multinuclear, high-resolution NMR study of bovine casein micelles and submicelles. Biophys. Chem. 38:87–98.

14 Krimm, S., and J. Bandekar. 1986. Vibrational spectroscopy and conformation of peptides, polypeptides, and proteins. Adv. Protein Chem. 38:181–364.
15 Kumosinski, T. F., and H. M. Farrell, Jr. 1994. Solubility of proteins: protein-salt water interactions. Pages 39–77 *in* Protein Functionality in Food Systems. N. S. Hettiarachchy and G. R. Zeigler, ed. Marcel Dekker, Inc. New York, NY.
16 Kumosinski, T. F., G. King, and H. M. Farrell, Jr. 1994. An energy-minimized casein submicelle working model. J. Protein Chem. 13:681–700.
17 Kumosinski, T. F., H. Pessen, H. M. Farrell, Jr., and H. Brumberger. 1988. Determination of the quaternary structural states of bovine casein by small-angle X-ray scattering: submicellar and micellar forms. Arch. Biochem. Biophys. 266:548–561.
18 Kumosinski, T. F., and J. J. Unruh. 1996. Quantitation of the global secondary structure of globular proteins by FTIR spectroscopy: comparison with X-ray crystallographic structures. Talanta 43:199–219.
19 Kumosinski, T. F., J. J. Unruh, and H. M. Farrell, Jr. 1997. Reproducibility of the nonlinear regression fit to the FTIR spectra of lysozyme. Talanta 44:1441–1445.
20 Rose, G. D., L. M. Gierasch, and J. A. Smith. 1985. Turns in peptides and proteins. Adv. Protein Chem. 37:1–109.
21 Schmidt, D. G. 1982. Associations of caseins and casein micelle structure. Pages 61–96 *in* Developments in Dairy Chemistry–1. P. F. Fox, ed. Appl. Sci. Publ., Ltd., Essex, United Kingdom.
22 Surewicz, W. K., H. H. Mantsch, and D. Chapman. 1993. Determination of protein secondary structure by FTIR: a critical assessment. Biochemistry 32:389–394.
23 Swaisgood, H. E. 1982. Chemistry of milk proteins. Pages 1–60 *in* Developments in Dairy Chemistry–1. P. F. Fox, ed. Appl. Sci. Publ., Ltd., Essex, United Kingdom.
24 Thompson, M. P. 1964. Phenotyping of caseins of cow's milk: collaborative experiment. J. Dairy Sci. 47:1261–1262.
25 Wahlgren, N. M., J. Leonil, P. Dejmek, and T. Drakenberg. 1993. Two dimensional NMR study of the β-casein peptide 1-25. Biochim. Biophys. Acta 1202:121–128.
26 Wilder, C. L., A. D. Friedrich, R. O. Potts, G. O. Daumy, and M. L. Francocur. 1992. Secondary structural analysis of two recombinant murine proteins, interleukins 1α and 1β. Biochemistry 31:27–31.
27 Yang, W. J., D. M. Griffiths, D. M. Byler, and H. Susi. 1985. Protein conformation by infrared spectroscopy: resolution enhancement by Fourier self-deconvolution. Appl. Spectrosc. 39: 282–287.